Eur. Phys. J. A **6**, 275–288 (1999)

THE EUROPEAN PHYSICAL JOURNAL A

Pre-equilibrium dipole excitation and γ-ray fragment angular correlation in the ^{32}S + ^{74}Ge reaction

M. Sandoli[1,2], A. Boiano[1], L. Campajola[1], A. De Rosa[1,2], A. D'Onofrio[3,1], G. Inglima[1,2], M. La Commara[4], A. Ordine[1], D. Pierroutsakou[1], V. Roca[1,2], M. Romano[1,2], M. Romoli[1], M. Trotta[1,2], F. Rizzo[5,6], F. Amorini[5,6], S. Tudisco[5,6]

[1] INFN, Sezione di Napoli, Napoli, Italy
[2] Università di Napoli "Federico II", Dipartimento di Scienze Fisiche, Napoli, Italy
[3] Seconda Università di Napoli, Facoltà di Scienze Ambientali, Italy
[4] GSI, Darmstadt, Germany
[5] Università di Catania, Dipartimento di Fisica, Catania, Italy
[6] INFN, Laboratorio Nazionale del Sud, Catania, Italy

Received: 24 March 1999 / Revised version: 17 May 1999
Communicated by D. Schwalm

Abstract. We report on the results obtained from the study of the ^{32}S $+^{74}$Ge deep inelastic reaction at incident energy $E = 320$ MeV. High-energy γ-rays were detected in an array of 6 seven-pack BaF_2 clusters. Coincidence with complex fragments detected in 12 three-stage telescopes ensured the selection of peripheral reaction events. In order to investigate the pre-equilibrium dipole strength excitation two independent analyses were performed. In the first analysis the energy spectra of the γ-rays were evaluated in the statistical model framework while in the second one the γ-ray fragment angular correlation with respect to the nuclear spin vector of the composite system was studied. Both methods indicate the excitation of dipole strength in the highly deformed dinucleus and provide dipole resonance parameter sets that are in good agreement with each other.

PACS. 25.70.-z Low and intermediate energy heavy-ion reactions – 24.30.Cz Giant resonances – 23.20.-g Electromagnetic transitions – 25.70.Lm Strongly damped collisions

1 Introduction

The study of the Giant Dipole Resonance (GDR) during the last decades was demonstrated to be a powerful tool in getting information on the structure of highly excited and rotating nuclei. From its first observation in proton capture experiments [1] up to now a large systematics was obtained on GDR excited in systems with different masses, temperatures and spins, mostly created in heavy-ion induced fusion, fusion-fission or quasifission reactions [2–7].

Besides the large body of data concerning rather equilibrated nuclei, formed at low excitation energies, the study of dipole strength in systems far from equilibrium was recently revealed of great interest. In fusion reactions the observation of the GDR disappearance for temperatures larger than 5 MeV [8-10] and the observation of extra strength in the γ-ray spectrum at energies 8 MeV $< E_\gamma <$ 12 MeV [8, 9] feeded many discussions. For the latter, among other hypotheses, the pre-equilibrium dipole strength excitation in charge asymmetric heavy-ion collisions emerged as a likely explanation [11-15].

To study nuclear systems far from equilibrium, peripheral reactions between heavy ions appear immediately to be the best candidate. The possibility to excite the dipole states of the composite system formed in such reactions was first suggested in studying the complex fragment charge distribution as a function of the total kinetic energy loss [16] while theoretically the enhancement of the E1 transitions was examined by deriving molecular sum rules [17]. Furthermore, from the study of the dissipative excitation functions it was shown that the too small number of final effective channels contributing to the dissipative cross section could be understood if considering a selective excitation of doorway states of the dinuclear system like the dipole ones [18].

In this framework we have started a research program based on the study of heavy-ion deep inelastic reactions. In previous works [19, 20], where the γ-rays were detected in coincidence with the complex fragments emitted in the ^{35}Cl $+^{64}$Ni and ^{35}Cl $+^{92}$Mo reactions, we evidenced that the energy spectra of the γ-rays cannot be completely explained by the fragment statistical decay. In these papers the excess of cross section with respect to that of the calculated spectra was attributed to the γ-decay of the composite system GDR, the so-called pre-equilibrium GDR.

In the present paper the GDR excitation in the charge asymmetric $^{32}S + ^{74}Ge$ reaction at incident energy of 320 MeV will be presented. The statistics of this experiment is greatly enhanced with respect to the previous ones allowing an analysis of the data in two different ways : a) within the framework of the statistical model, where various approaches were tested in order to verify the obtained results; b) by studying the γ-ray fragment angular correlation.

In Sect. 2 we present the experimental methods, in Sects. 3, 4 and 5 the γ-ray energy spectra and the analysis within the statistical model framework, while in Sects. 6 and 7 we study the γ-ray fragment angular correlation. The conclusions are presented in Sect. 8.

Before describing the experimental methods and the data analysis, it is useful to clarify the term "pre-equilibrium dipole strength" often appearing in the text. From a phenomenological point of view, in the early stages of a heavy-ion deep inelastic collision a highly deformed system is created, the dinucleus or intermediate system, which under the influence of a high Coulomb and centrifugal barrier breaks up into two masses similar to those of the colliding ions. Its lifetime depends on the collision impact parameter and spans from $1{\cdot}10^{-21}s$ to $5{\cdot}10^{-21}s$ for fragmentations near and far from that of the entrance channel respectively [21]. During this time the various degrees of freedom proceed towards relaxation, some among them never attaining complete equilibrium. For instance, the shape of the intermediate system remains highly deformed up to fragmentation. That implies a treatment of the γ-ray emission from the dinucleus different from that of a completely equilibrated system. Roughly speaking, the γ-ray spectrum originating from the intermediate system created in a charge asymmetric collision should contain a pre-equilibrium dipole component and an equilibrium dipole one with respect to the dipole moment relaxation ($\sim 10^{-22}$ s). In the case of charge symmetric collisions only the equilibrium component should be present. However, according to the previous discussion, both dipole components are of pre-equilibrium character with respect to the shape relaxation and/or other degrees of freedom. By pre-equilibrium dipole strength in this work we shall mean dipole strength excited in a nucleus prior to its complete equilibration. In order to avoid confusion, we note that in the existing bibliography the term pre-equilibrium GDR is mainly used to describe the dipole component existing at the beginning of a charge asymmetric collision.

Since in the present reaction there is a relatively large entrance channel charge asymmetry $\Delta\left[\left(\frac{N}{Z}\right)_{targ} - \left(\frac{N}{Z}\right)_{proj}\right] = 0.31$, both contributions could exist though it is not possible to isolate them experimentally.

2 Experimental methods

The reaction was performed by using the 320 MeV pulsed beam of ^{32}S provided by the superconducting heavy-ion linear accelerator of the Laboratori Nazionali di Legnaro (Italy), impinging on a 500 μg/cm^2 thick ^{74}Ge target. The beam consisted of $\sim$2 ns wide bunches with a 200 ns separation. The beam intensity was measured in a Faraday cup shielded with lead and paraffin to reduce the background due to γ-rays and neutrons.

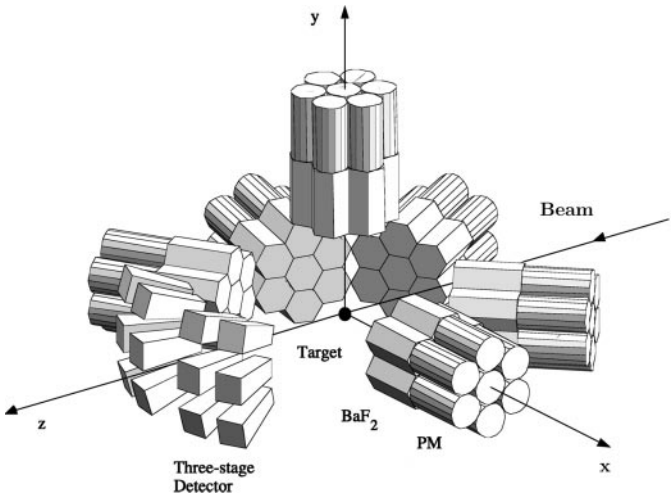

Fig. 1. Experimental set up

The γ-rays were detected by using 6 seven-pack clusters of BaF_2 scintillators of the TAPS standard situated at 30 cm from the target and at the following (θ, ϕ) angles with respect to the beam direction taken to coincide with the Oz axis: (72.5°, 180°), (90°, 90°), (90°, 0°), (112.5°, 180°), (132.5°, 0°), (152.5°, 180°). The total solid angle covered by the BaF_2 detectors was 11% of 4π. The scintillators were surrounded by a 3 mm thick lead shield which reduced the counting rate due to the low-enegy γ-rays ($E_\gamma \leq 1$ MeV) to 50% and stopped the charged particles.

The reaction products were detected and charge identified by means of an array of 12 three-stage detectors each consisting of a gas ionization chamber, a silicon detector and a CsI(Tl) scintillator. This array was described in detail in [22]. The fragment detectors were placed at 35 cm from the target in the forward hemisphere with respect to the beam direction, covering the angular range between 11° and 37° and including the laboratory grazing angle $\theta_{gr} = 14.6°$. Their total solid angle was 0.144 sr. The experimental set up is shown in Fig. 1.

Coincidence events between a particle detector and at least one fired BaF_2 scintillator were collected during the experiment. An event was accepted if the deposited energy in a BaF_2 cluster was greater than $\sim$5 MeV. The threshold of the BaF_2 scintillators was set at $\sim$100 keV. The coincidence request eliminated any cosmic ray contamination of the γ-ray spectra.

The discrimination between γ-rays and neutrons was performed by means of a measurement of the time of flight relative to the beam burst.

The energy calibration of the γ-ray detectors was obtained by using the sources ^{60}Co, ^{88}Y and the composite sources of $^{241}Am + ^{9}Be$ and of $^{238}Pu + ^{13}C$. The time stability of the energy calibration was verified during the experiment by controlling the stability of the peak corre-

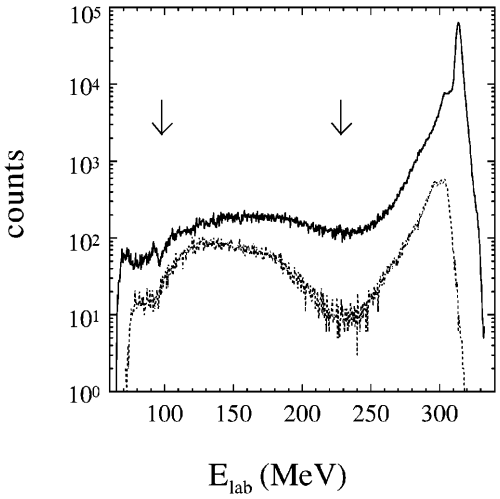

Fig. 2. Laboratory kinetic energy spectrum of the $Z = 16$ fragments emitted at $\theta_{lab} = 14°$ and $19°$. The events having energies included by the arrows were accepted in the analysis

sponding to a radioactive source. The energy calibration of the Si detectors was performed by using the elastic scattering of ^{32}S on various targets and the punch-through of the α particles, while the energy calibration of the ionization chamber was made by changing the gas pressure.

3 Results and ingredients of the analysis

In order to study the γ-ray energy spectra for inelastic events which do not lead to quasifission or fusion-fission, in the off-line analysis only γ-rays in coincidence with secondary fragments having charge between 10 and 18 were considered. Furthermore, fast quasi-elastic reactions were discarded. That was performed by selecting in the laboratory kinetic energy spectra of the detected fragment events with exit channel energies included in the dissipative bump. An example of such a selection is shown in Fig. 2 where the laboratory kinetic energy spectrum of the $Z = 16$ fragments emitted at $\theta_{lab} = 14°$ and $19°$ is presented. The events having kinetic energies situated between the arrows were accepted in the analysis.

In Fig. 3 the resulting cumulative γ-ray spectrum is reported with the points. The γ-rays mainly originate from the excited primary fragments but emission from the intermediate system prior to fragmentation is also expected according to results for other systems [19, 20]. From these γ-ray sources only the complex fragments can be taken as completely equilibrated nuclei and their γ-ray spectra can be calculated within the statistical model framework. In the following, the most important ingredients necessary for the statistical model calculation will be presented.

Since the mass of the ejectile was not measured, the initial fragment masses were deduced by choosing the most probable isotope of each element following the Q_{gg} systematics. The angular momentum $\hbar L_f$ transferred to the exit channel was obtained according to the sticking model

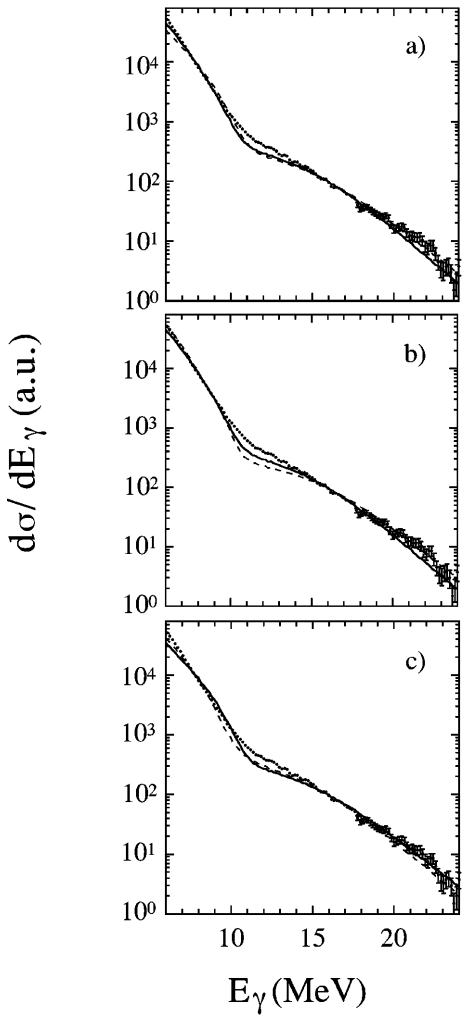

Fig. 3. The points in the three panels represent the cumulative experimental γ-ray spectrum while the lines correspond to the best fit curves of the data obtained by using the statistical model code CASCADE and by changing the following parameters: a) Solid line: Calculation performed in the equal temperature limit with a total excitation energy decreased by 20 MeV and with a level density parameter $a = A/8$. Dashed line: As the solid line but the total excitation energy was taken without any subtraction. b) Solid line: Identical to the solid line of a). Dashed line: Calculation performed in the equal temperature limit with a total excitation energy decreased by 20 MeV and with a temperature dependent level density parameter according to [36]. c) Solid line: Identical to the dashed line of a). Dashed line: Calculation performed in the hypothesis of an equipartition of the excitation energy between the fragments, with a total excitation energy taken without any subtraction and by using a level density parameter $a = A/8$

which is appropriate for deep inelastic events [23]:

$$\hbar L_f = \hbar L_i \frac{J}{(J + J_1 + J_2)} \quad (1)$$

with J and J_i the moment of inertia of the intermediate system and of the ith fragment respectively. The entrance

channel angular momentum $\hbar L_i$ was taken equal to:

$$\hbar L_i = \hbar \left[L_{cf} + 0.66 \left(L_{gr} - L_{cf} \right) \right] \tag{2}$$

L_{gr} being the grazing value and L_{cf} the critical value for fusion-evaporation. The partition of the total dissipated angular momentum, $\hbar(L_i\text{-}L_f)$, between the fragments was performed according to their moment of inertia. In the present experiment $L_{gr} = 144\hbar$, $L_{cf} = 58\hbar$ and $L_i = 115\hbar$.

The most probable exit channel center of mass kinetic energies corrected for particle evaporation can be decomposed according to the following equation:

$$E_{out} = \frac{L_f(L_f+1)}{2\mu R^2} + V_C(R) \tag{3}$$

with R being the distance between the two charge centers, μ the reduced mass of the composite system and $V_C(R) = \frac{e^2 Z_1 Z_2}{R}$ the Coulomb barrier at R. The (3) is valid when the radial velocity at this point can be neglected. In this way a distance R is defined outside of which the relative motion is subject to the conservative forces only. We can deduce R from the Coulomb repulsion of the primary fragments following the Viola systematics [24]. In the present case the separation of the charge centers at the scission moment is estimated to be $R = 13$ fm.

The distance R was used to obtain the moment of inertia of the composite system at the scission point and to calculate L_f from the sticking condition (1). In this calculation the fragments were considered as axially symmetric rigid spheroids with symmetry axis length $2a_i$ and perpendicular axis length $2b_i$. Then, their moments of inertia were approximated as following [25]:

$$\frac{J_i}{\hbar^2} = \frac{M_i}{197^2} \left\{ 2 + 0.2 R_i^2 \left[\left(\frac{a_i}{b_i} \right)^{\frac{4}{3}} + \left(\frac{b_i}{a_i} \right)^{\frac{2}{3}} \right] \right\} (MeV)^{-1} \tag{4}$$

$R_i = 1.22 A^{1/3}$ being the sharp-surface radius of a sphere having the same volume as that of the rigid spheroid and M_i the fragment mass. The ratio a/b of the fragment semi-axes was adjusted to give the correct experimental exit channel kinetic energies. It is worthnoting that the large deformation of the fragments at the scission point, necessary to reproduce the exit channel kinetic energies, disappears after their separation and their deformation is defined by their angular velocity according to the theory of the liquid drop.

To deduce the total excitation energy E^* of the primary fragments in the assumption of a binary reaction by knowing the laboratory kinetic energy and the charge of the detected secondary projectile-like fragments a procedure was used in which the particle evaporation was taken into account. The total excitation energy can be written:

$$E^* = E_{in} + Q_{gg} - E_{out} \tag{5}$$

where E_{in} and E_{out} are the center of mass kinetic energy in the reaction entrance and exit channel and Q_{gg} is the ground state Q value.

The excitation energy sharing among the primary fragments was done proportionally to their masses according to a thermal equilibrium hypothesis at the fragmentation moment. Such a choice should be reasonable as only deep inelastic events were considered in the analysis, however, in order to estimate the induced uncertainty different considerations will be made in the following.

For the present reaction the total center of mass energy is equal to $E_{in} = 223$ MeV and the most probable excitation energy shared between the primary fragments is found to be $E^* \sim$140 MeV. In the scenario of thermal equilibrium for masses between $A = 23$ and 83, the fragment excitation energy ranges from 22 to 118 MeV, the spin from $J = 4\hbar$ to $29\hbar$ and their temperature lies between 2.8 and 3 MeV.

The γ-ray spectrum of each considered fragmentation was calculated by using the code CASCADE [26, 27]. While for the target-like nuclei ($A \sim$74) the usual isospin independent version was considered sufficient to describe their statistical decay, for the projectile-like nuclei ($A \sim$32) an isospin dependent version [28] was used. In these calculations the isospin mixing was neglected since for nuclei with similar mass it was found to be small [28].

In the statistical calculations for the projectile-like fragments the GDR centroid energy was taken to be lower than that of the ground state GDR [29] since in heavy-ion collisions only the $T_< = T_z$ component of the GDR is populated. The centroid energy expected for the $T_<$ dipole component was calculated according to the relations given in [30, 31]. The total GDR strength found to be exhausted in (γ, n) and (γ, p) reactions was supposed to be exhausted by only the $T_<$ dipole component in the present reaction according to the results of Kicinska-Habior et al. [32, 33].

However, for the target-like fragments the GDR centroid energy was taken to be equal to that of the ground state (g.s.) GDR. The reason for that is to be found in their g. s. GDR characteristics. For example, the g. s. GDR resonance excited in the ^{74}Ge is well fitted in [29] by using two lorentzian curves with strength ratio $S_2/S_1 = 18.2$ and with an energy separation of $\Delta E = 2.5$ MeV. In the case of a GDR splitting due to the isospin, a ratio $S_2/S_1 = S_>/S_< \sim 0.1$ is expected and a separation of the dipole components $\Delta E \sim$5 MeV [30, 31, 34, 35]. The comparison shows that the ground state GDR splitting is a nuclear deformation effect rather than an isospin one. The same stands for all nuclei in this mass region ($A \sim$74).

The fragment GDR width was taken from the existing systematics [2, 3, 4, 8, 10, 27, 32, 33]. Experimentally it was observed that the GDR width increases with increasing the nuclear excitation energy up to a value where a saturation of the width occurs. For isotopes of Sn the experimental relation which reproduces the evolution of the width with the excitation energy $E^*$is [3]: $\Gamma_{GDR} = \Gamma_0 + 0.0026 * E^{*1.6}$ with Γ_0 the ground state GDR width. For masses near 100 and 136 the width saturation has been observed at $E^*/A \sim$1.2 MeV [4]. In the present paper, we used a GDR width given at the considered excitation energies from the above experimental relation, saturating at an excitation energy $E^* = (1.2\ A)$ MeV and with the

ground state value Γ_0 obtained from the photoabsorption data [29]. The width was kept constant throughout the decay chain of each primary fragment.

Another important element of the calculations concerns the level density parameter which unfortunately is not well known at high excitation energies. Since its influence on the calculated spectra could be important, in the analysis two different approaches were tested: a constant level density parameter $a = A/8$ and a temperature dependent one. For the temperature dependent level density parameter the following formula [36] was used:

$$a(T) = \frac{A\left[1 + 0.4\exp\left(-\frac{T^2}{9}\right)\right]}{k} \qquad (6)$$

The exponential temperature dependence of a is due to small amplitude quantal fluctuations of the nuclear surface. The coefficient k reflects nuclear surface large amplitude thermal fluctuations and it is relatively stable with the mass, the angular momentum and the temperature of the nuclei. To give an example, its value ranges from 11.3 to 11.6 for masses $67 < A < 83$, spins $20\hbar < J < 29\hbar$ and temperatures $0 < T < 2$ MeV. From the (6) we deduce $a = A/8.4$ at $T = 1$ MeV and $a = A/10$ for $T = 3$ MeV. The level density parameter saturates for temperatures $T \sim 5$ MeV at the value $a = A/k$. As it was shown in [27], the use of a temperature dependent a rather than of $a \sim A/8 - A/9$ causes an increase of the extracted nuclear temperature and influences the γ-ray spectrum.

The Isoscalar and Isovector Giant Quadrupole Resonances (ISGQR and IVGQR) of the fragments were also taken into account [37, 38], however their influence is quite small in the energy range between $E_\gamma = 6$ and 22 MeV. For the emission of magnetic dipole radiation a constant strength ξ was used with an energy dependence $\xi_J = E_\gamma^{2J+1}$ which is the basic energy dependence for single particle transitions [39]. All the theoretical γ-ray spectra were folded by the experimental set up response function by using the code GEANT3 [40].

The Doppler shift correction due to the motion of the fragments in the laboratory reference frame was also considered. As it was impossible to perform an event by event treatment because of the ambiguity of the γ -ray source, the reverse procedure was followed by transforming in the laboratory frame the statistical γ-ray spectra of the fragments initially calculated in their respective center of mass. To this aim, the calculated γ-ray spectrum in coincidence with each fragment detector and each BaF_2 cluster was determined separately and then the total γ-ray spectrum relative to each fragment was obtained by summing all the individual spectra with the experimental weight of the corresponding particle detector. The correction was performed by using the following equations: $\sin\theta_{cm} = \frac{\sin\theta_{lab}}{\gamma(1-\beta\cos\theta_{lab})}$, $E_{cm} = E_{lab}\gamma(1 - \beta\cos\theta_{lab})$

$$\frac{d^2\sigma(\theta_{cm}, E_{cm})}{dE_{cm}d\Omega_{cm}} = \frac{d^2\sigma(\theta_{lab}, E_{lab})}{dE_{lab}d\Omega_{lab}}\gamma(1 - \beta\cos\theta_{lab}) \qquad (7)$$

$$\gamma = \frac{1}{\sqrt{1-\beta^2}}, \quad \beta = \frac{v}{c}$$

where θ_{lab} and θ_{cm} are the angles between the γ-ray direction and the velocity vector $\mathbf{v}$ of the emitting source in the laboratory and in the source center of mass frame respectively. It was found that the Doppler shift correction is negligible for the cumulative γ-ray spectrum as a consequence of the fact that the distribution of the angles between particle and γ-ray detectors was symmetrical around 90°.

Among the different mechanisms which may feed the γ-ray spectra at energy $E_\gamma > 20$ MeV the nucleon-nucleon bremsstrahlung should be the dominant one [41]. At the present incident energy it represents no more than 15% of the γ-ray cross section at $E_\gamma = 20$ MeV. As it affects in a small way the energy region between 10 and 15 MeV we have neglected its contribution in the analysis.

Since no information exists on the relative cross section of the initial fragmentations, we have deduced those mainly contributing to the cumulative γ-ray spectrum in the following way: the two experimental γ-ray spectra obtained in coincidence with final projectile-like fragment charges varying from $z_{fin} = 10$ to $z_{fin} = 14$ and from $z_{fin} = 15$ to $z_{fin} = 18$ were considered separately. Then, these spectra were fitted, by means of a least square procedure, over the whole energy range of the data, by using a linear combination of the cross section of the feeding initial fragmentations. In the fitting procedure, the weight of the statistical spectrum associated with each feeding fragmentation was free while all other parameters used in the CASCADE code were kept constant. In order to take into account the exponential nature of the γ-ray spectra we have minimized the χ^2 divided by the number of counts at each energy bin.

4 Comparison of the data with statistical model calculations

In all panels of Fig. 3 the experimental cumulative γ-ray spectrum is shown with the points and the different calculations with the lines. Each calculated cumulative γ-ray spectrum corresponds to the best fit of the data regarding the relative weight of the initial fragmentations and to a fixed choice of the parameters used in the CASCADE code. In Sect. 3 we have described the initial choice of these parameters, then, in the following we are discussing only the value of those which will be changed, the other remaining constant as described in Sect. 3. Among the calculated γ-ray spectra corresponding to different choices of the statistical model parameters, the one having the minimum χ^2 divided by the number of counts at each energy bin in the energy range between $E_\gamma = 6$ MeV and $E_\gamma = 20$ MeV will be indicated later in the text.

The dashed line of Fig. 3a corresponds to a calculation performed by using in the code CASCADE a constant level density parameter $a = A/8$ throughout the decay chain. The data are well fitted at both low and high energy, however between 10 and 15 MeV the theoretical spectrum underestimates the γ-ray yield. If, instead of $a = A/8$, another constant value of the level density parameter is

used, like $a = A/9$, $A/10$, $A/11$, the quality of the fit at this energy region worsens.

The fit becomes slightly better at low energies if, in addition to the use of $a = A/8$, 20 MeV are subtracted from the total excitation energy E^* shared between the fragments (solid line of Fig. 3a). A small amount of this energy could be explained by the deformation of the fragments. To give an example, the fragments of mass $A_1 = 31$ and $A_2 = 75$ for spins $J = 7\hbar$ and $26\hbar$ respectively should have oblate noncollective shapes with equilibrium deformations $\beta_{eq} = 0.07$ and $\beta_{eq} = 0.16$ [42] and rotational frequency at the equilibrium configuration $\omega_{rot} = 1.3$ MeV. To obtain the equilibrium deformation of the fragments which minimizes the free-energy F at temperature T and rotational frequency ω_{rot}, we assumed that at $T \sim$2.5 - 3 MeV the shell corrections included in F are small and the nuclei behave like a liquid drop. The corresponding total deformation energy of the fragments is found to be $E_{def} = 3$ MeV, too small with respect to 20 MeV. A valid reason for decreasing the total excitation energy by 20 MeV could be the emission of a particle or γ-ray prior to the composite system fragmentation. What is important to notice is that both calculations, with and without any energy subtraction, underestimate the experimental γ-ray yield between 10 and 15 MeV. To ensure ourselves that this γ-ray excess with respect to the statistical calculations is real and does not reflect some bias in the statistical model parameters, different hypotheses were examined.

By keeping the total excitation energy decreased by 20 MeV and by using a temperature dependent level density parameter [36] (dashed line of Fig. 3b) the γ-ray excess with respect to the calculation gets even larger than it did previously. For comparison the solid line of Fig. 3a was also reported in Fig. 3b.

The GDR width of the fragments was varied in order to verify whether the quality of the fit can be improved. For γ-ray energies larger than 10 MeV the target-like fragment spectrum dominates. By changing the target-like fragment GDR width from $\Gamma = 11$ MeV up to $\Gamma = 15$ MeV, we do not significantly improve the fit while with a larger width, the high energy part of the data can be no more reproduced. Furthermore, the variation of the GDR centroid energy for both the target and the projectile-like fragments within $\pm$1 MeV and of the GDR strength within $\pm$ 0.1 TRK does not change the results. The same holds if the spin of the fragments was changed within $\pm 2\hbar$ and $\pm 5\hbar$ for the projectile-like and the target-like fragment respectively.

Another parameter which could introduce uncertainty is the excitation energy sharing between the primary fragments. By looking at the existing bibliography one can see that recent papers [43-46] converge that for partially damped events the excitation energy is equally partitioned between the fragments while for more relaxed ones the energy partition tends to become proportional to the fragment mass ratio. In the previous calculations an equal temperature of the fragments was assumed. In order to estimate the uncertainty due to this hypothesis, calculations were also made by assuming an equipartition of the excitation energy for fragmentations similar to the entrance channel one and $E^*_{PLF} = 0.6E^*_{tot}$ for those with a larger amount of transferred nucleons according to recent results on the excitation energy sharing [46]. The result is shown by a dashed line in Fig. 3c, while the solid line in the same panel (identical to the dashed line of Fig. 3a) corresponds to a partition proportional to the mass ratio. In both calculations the total excitation energy of each fragmentation was taken without any subtraction and a constant level density parameter $a = A/8$ was used. The difference of these two curves is small in the energy range of interest, i.e. between 10 and 15 MeV, mainly consisting in a displacement of the γ-ray excess towards smaller energies. Although none of these energy sharing limits is realistic, the system should be nearer to the equal temperature limit as far as deep inelastic events are concerned. Then, as the results on the γ-ray excess are not much altered by this choice the hypothesis of an equal temperature of the fragments was maintained.

To summarize, the previous attempts to fit the entire experimental γ-ray spectrum by changing the statistical model parameters showed that, although we are able to reproduce the data at both low and high energies, the fit drops in the range between 10 and 15 MeV where all calculations underpredict the γ-ray yield (see the different curves of Fig. 3). We recall that some difference between data and calculations at energies larger than 20 MeV is due to the nucleon-nucleon bremsstrahlung γ-ray emission which was not taken into account in the analysis. The evidenced γ-ray excess in the range between 10-15 MeV can be better seen in both panels of Fig. 4b where the ratio between the data and the calculations is displayed by the points. To obtain this ratio, in the left-hand side of the Fig. 4b the calculation presented with a dashed line in the Fig. 3a was used while in the right-hand side the calculation corresponds to the solid line of the Fig. 3a.

5 Discussion I

A similar fit of the data was also obtained in [19, 20] where the observed γ-ray excess was attributed to the γ-decay of a dipole oscillation present in the dinucleus during the sticking time.

In a deformed non rotating system the dipole resonance splits in three components corresponding to vibrations along the three principal axes, with energies inversely proportional to the associated axis length. For a collectively rotating prolate shape the Coriolis forces and the transformation from the internal to the laboratory frame cause a further splitting of the dipole resonance which is proportional to ω_{rot} [47]. In the case of a non collectively rotating oblate shape the final result in the laboratory frame is the same as for $\omega_{rot} = 0$ [47]. As for heavy systems with $A \sim$100, ω_{rot} lies between 1 and 1.5 MeV such a splitting can be considered small and so can be neglected.

In the present case the high energy part of the experimental γ-ray spectrum is well accounted for by only the statistical spectra of the fragments. Then, the γ-ray excess

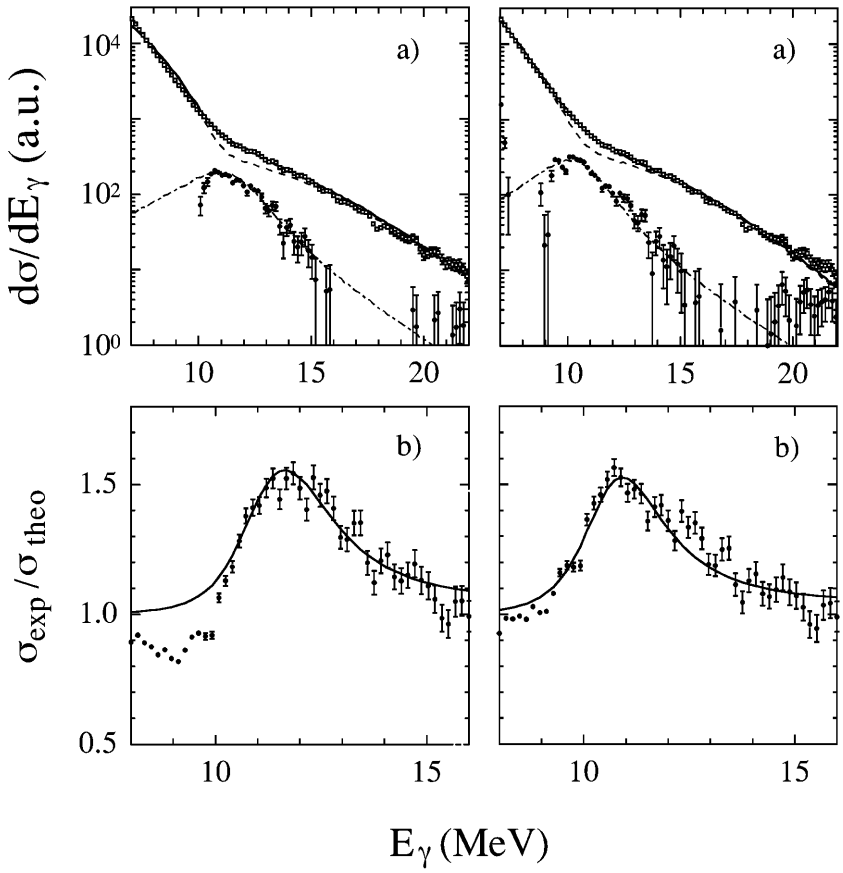

Fig. 4. a) Cumulative experimental γ-ray spectrum (open symbols), statistical spectrum of the fragments (dashed line) and their difference (filled symbols). The dot-dashed line is a calculation representing the dinucleus γ-ray spectrum and is obtained as described in the text. The solid line corresponds to the sum of the dinucleus γ-ray spectrum and that of the fragments. Left hand-side column: the statistical γ-ray spectrum is identical to that displayed by the dashed line in Fig. 3a. Right hand side column: the statistical spectrum corresponds to that displayed by the solid line in Fig. 3a. b) Ratio of the cumulative experimental γ-ray spectrum and the statistical one (points). The solid line corresponds to the sum of the dinucleus γ-ray spectrum and that of the fragments divided by this latter

evidenced in the range between 10 and 15 MeV should correspond to the low energy dipole oscillation along the symmetry axis of the dinucleus in the direction of the collision. The above result does not exclude the existence of some dipole strength at high energies but it indicates that such a strength should be much less than that observed at $E_\gamma = 12$ MeV, rendering its extraction difficult as at high energies the GDR of the fragments dominates. At first sight the fact that only the low-energy dipole component is observed appears to be strange but a possible explanation could be searched in the entrance channel charge asymmetry. According to recent papers [12, 15], if there is an asymmetry in the N/Z degree of freedom between the colliding ions, a "direct" dipole mode is present at $t = 0$, in the collision direction, associated with the charge equilibration between the ions occuring during the first $\sim$ 200 fm/c. Along the shorter axes of the composite system dipole oscillations can exist after $\sim 10^{-22}$ s which is the time necessary for the GDR to be excited. Therefore, it is likely that the low energy dipole component associated with the oscillation along the rotating maximum elongation axis of the composite system is significantly larger than the higher energy components. However, this point will be further discussed in Sect. 7.

Since at the moment no appropriate model exists for describing the GDR γ-ray emission from systems far from complete equilibrium as is the case of the composite system formed in heavy-ion deep inelastic scattering, the evidenced γ-ray excess cross section $\sigma_{pre}(E_\gamma)$ was approximated by the following expression:

$$\sigma_{pre}(E_\gamma) = N' \sum_i f_i(E_\gamma) \exp(-cE_\gamma) \qquad (8)$$

where N' is a normalization factor and $f_i(\mathrm{E}_\gamma)$ is the strength function of the ith dipole component in a hot nucleus:

$$f_i(E_\gamma) = 2.09 \times 10^{-5} \frac{NZ}{A} \frac{S_i \Gamma_i E_\gamma^4}{\Gamma_i^2 E_\gamma^2 + (E_i^2 - E_\gamma^2)^2} \qquad (9)$$

E_i, Γ_i and S_i being respectively the energy, the width and the fraction of the TRK energy weighted sum rule (EWSR) exhausted from the i^{th} dipole component. The exponential function in (8) is an approximation used in the statistical γ-ray emission for taking into account the ratio between the nuclear level density of the final and initial nuclear state:

$$\frac{\rho(E_{fin})}{\rho(E_{in})} \quad \propto \quad \exp(-cE_\gamma) \qquad (10)$$

In the case of a non statistical emission the level density dependence on E_γ could be different. Then, the above procedure should be considered as a fit to the data and the extracted parameters should be taken with caution. The curve of (8) was folded by the experimental set up response function using the code GEANT3 [40].

The γ-ray excess, although present in all cases (see Fig. 3), shows some differences depending on the theoretical γ-ray spectrum of the fragments used for the comparison. To give an idea, in Fig. 4a two of the four calculated statistical γ-ray spectra are reported with the dashed lines as explained previously for the Fig. 4b. The open symbols of Fig. 4a correspond to the cumulative experimental γ-ray spectrum while the filled symbols represent the difference between the data and the relative fragment statistical γ-ray spectrum. The dot-dashed line is the result of the above procedure using the (8) and corresponds to the dinucleus γ-ray spectrum. The solid line results from the sum of the statistical γ-ray spectrum of the fragments and the dinucleus γ-ray spectrum and reproduces well the data in the whole energy range. The ratio of Fig. 4b is also well described when dividing this sum by the respective statistical γ-ray spectrum of the fragments.

The parameters in (8) used for the case presented on the left-hand side column of the Fig. 4 (no excitation energy subtraction) are : E_1 = 12 MeV, Γ_1 = 3 MeV, c = 1/3 (MeV)$^{-1}$. In the case of 20 MeV subtraction from the total excitation energy (right hand-side column of the figure) the centroid energy shifts down to E_1 =11 MeV, the width becomes Γ_1 = 2.5 MeV while the ratio between the data and the relative theoretical γ-ray spectrum does not change as can be seen from Fig. 4b.

Since using the latter theoretical γ-ray spectrum of the fragments we obtain the best fit of the data (cf. Fig. 4), in the following we will retain this calculation and the associated parameter set : E_1 = (11± 1) MeV, Γ_1 = (2.5± 0.5) MeV, c = 1/3 (MeV)$^{-1}$. The uncertainty of the statistical model parameters was also taken into account in the errors.

The extracted resonance energy is in a good agreement with the oscillation energy E_D of a dipole having as major semi-axis length the sum R_S of the colliding ion radii calculated according to the empirical formula:

$$E_D \approx \frac{78}{\left(A_1^{1/3} + A_2^{1/3}\right)}\ MeV = 10.6\ MeV \qquad (11)$$

with A_1 and A_2 being the masses of the colliding ions. It is interesting to note that the deduced low-energy component width is comparable with its ground state value, $\Gamma_i = \Gamma_0 \left(\frac{E_i}{16}\right)^{\delta}$ with E_i being the energy of the ith dipole component, δ ∼1.8 and Γ_0 = 6 MeV the ground state value of the GDR width built on a spherical nucleus of mass A = 106. That is another common element with the results published in [19, 20]. A similar observation can also be found in [7].

A detailed discussion on the GDR width can be found in [20, 48] so in this paper we recall briefly its main aspects. As known, the GDR width increases with the nuclear excitation energy because of the GDR coupling with the quadrupole surface degrees of freedom. The nuclear equilibrium deformation increases with spin, thus resulting in a larger GDR width [49-51]. On the other hand, while at zero temperature the deformation is determined by the quadrupole shape parameters β and γ which minimize the potential energy, at finite temperature there is a distribution of deformations caused by the nuclear surface thermal fluctuations which also contributes to the broadening of the GDR width [52, 53].

In the case of deep inelastic collisions it was shown [20, 48] in the framework of the Strutinsky model [54, 55] that there is a strong selection of the reaction initial angular momentum resulting in a limitation of the number of deformations that the system experiences. Moreover, the width broadening due to the nuclear surface thermal fluctuations should be reduced in the case of a system far for shape equilibrium due to the limitation of the deformations that the system can explore without undergoing fragmentation. Then, the GDR width should reflect a limited number of deformations around a central value of β. The fact that the composite system deformation is expected to be large should render the dipole components rather separated from each other with respective widths comparable to those of the ground state.

6 The γ-ray fragment angular correlation

An alternative method to investigate pre-equilibrium dipole γ-rays emitted from hot and rotating systems, immune to the uncertainties of the statistical model parameters, consists in the study of the γ-ray fragment angular correlation. The center of mass double differential cross section for detecting in coincidence a γ-ray and a complex fragment b in a peripheral heavy-ion collision can be written [56]:

$$\frac{d^2\sigma}{d\Omega_\gamma d\Omega_b} \propto \frac{d\sigma}{d\Omega_b}\ \frac{W(\mathbf{k}_\gamma)}{4\pi} \qquad (12)$$

where the angular correlation function $W(\mathbf{k}_\gamma)$ is the relative probability of the γ-ray being emitted in the direction $\mathbf{k}_\gamma$:

$$\begin{aligned} W(\mathbf{k}_\gamma) &= W(\theta,\phi) \\ &= \sum_k A_{k0} P_k(\cos\theta) + 2\sum_k \sum_{q>0} [(\mathrm{Re}\, A_{kq})\cos(q\phi) \\ &\quad -(\mathrm{Im}\, A_{kq})\sin(q\phi)] C_{kq}(\theta,0) \end{aligned} \qquad (13)$$

with θ and ϕ the center of mass polar angles of the γ-ray momentum $\mathbf{k}_\gamma$ with respect to some set of axis, $P_k(\cos\theta)$ the Legendre polynomial of degree k and C_{kq} is related to the associated Legendre functions:

$$C_{kq}(\theta,0) = (-)^q \left[\frac{(k-q)!}{(k+q)!}\right]^{1/2} P_k^q(\cos\theta) \quad if\ q \geq 0$$

The coefficients A_{kq} are constructed so that $A_{00} = 1$.

In the present case we choose as quantization axis, Oz // $\mathbf{k}_a \times \mathbf{k}_b$, $\mathbf{k}_a$ and $\mathbf{k}_b$ being the incident particle and the detected projectile-like fragment momenta which determine the reaction plane. The total angular momentum $\mathbf{J}$ of the created composite system is equal to the vector sum of the entrance channel spin $\mathbf{S}$ and of the ingoing orbital angular momentum $\mathbf{L}_o$: $\mathbf{J} = \mathbf{L}_o + \mathbf{S}$. As $\mathbf{S}$ is zero and $\mathbf{L}_o$ is

perpendicular to the reaction plane, **J** coincides with the quantization axis. In the hypothesis of parity conservation and of no interference between opposite parity γ-ray emitting nuclear states, in the γ-ray fragment angular correlation function only even order k terms with $q = 0$ survive. The same holds even when more initial nuclear states are present at the considered excitation energy provided that the decaying system is equilibrated. In that case, according to the Bohr theorem, the hypothesis of the absence of phase correlations between the nuclear states requires that interference terms between different reaction amplitudes vanish when averaging over initial states. Then, (13) reduces to:

$$W(\theta) = \sum_{k\ even} A_{k0} P_k(\cos\theta) = 1 + \sum_{k\ even \geq 2} a_k P_k(\cos\theta) \qquad (14)$$

$$a_k = A_{k0}$$

On the contrary, if the system is not equilibrated and opposite parity initial states interfere, also odd order k terms and terms with $q \neq 0$ enter the angular correlation.

The maximum order of the Legendre polynomials in (14) is given from the condition $k \leq 2L_{max}$ with L_{max} the maximum angular momentum of the contributing radiations. At the γ-ray energies of interest here, 8 MeV $< E_\gamma <$ 16 MeV, the electric dipole radiation (E1) dominates and the development in (14) could stop at the term of order $k = 2$. In the high spin limit and for statistical γ-ray emission the coefficient a_2 becomes:

$$m = \pm 1 \longrightarrow a_2 \approx 1/2$$

$$m = 0 \longrightarrow a_2 \approx -1$$

with m the projection of the dipole photon angular momentum on the spin axis. Dipole transitions with $m = 0$ are called unstretched transitions and correspond to $J_{in} = J_{fin}$, J_{in} and J_{fin} being the initial and final state spins, while the transitions with $m = \pm 1$ are called stretched transitions and correspond to $J_{in} = J_{fin} \pm 1$. Then, in the case of a spherical nucleus the angular distribution of statistical high energy γ-rays should be nearly isotropic as the final states are averaged over spin and the final state level density is a linear function of the nuclear spin. But if the system is deformed, an anisotropic emission of the high energy γ-rays is expected due to the energy splitting caused by the deformation. The resulting anisotropy depends on the deformation type (prolate or oblate), on the deformation magnitude and on the orientation of the symmetry axis with respect to the rotational axis.

For a prolate shape rotating collectively, as should be the case for the dinucleus formed in a peripheral collision, the symmetry axis is perpendicular to the rotational axis which in our case coincides with the quantization axis. Then, the low energy dipole component which corresponds to a vibration along the symmetry axis of the system corresponds to an $m = \pm 1$ dipole transition with respect to the rotational axis while the high energy dipole ones are associated with vibrations along the two short axes and are an equal mixture of $m = 0$ and $m = \pm 1$ transitions. In the case of a non collectively rotating oblate shape the rotational axis coincides with the symmetry axis. Then, the low energy dipole components which correspond to vibrations along the two axes perpendicular to the rotational axis are associated with $m = \pm 1$ dipole transitions while the high energy dipole component corresponds to a vibration along the symmetry axis and then it is associated with an $m = 0$ dipole transition.

In the present experiment the γ-ray fragment angular correlation was measured by using the BaF_2 clusters in coincidence with different fragment detectors. The existence of anisotropy in the γ-ray emission can be seen in the ratio of the experimental γ-ray spectra obtained at different angles with respect to the rotational axis. Such a ratio is displayed by the points in the left-hand side column of the Fig. 5. Due to the lack of measurements of singles deep inelastic events, the experimental γ-ray yields were normalized at $E_\gamma = 7$ MeV to the statistical spectrum of the primary complex fragments, calculated for the considered angles. The theoretical spectrum is corrected for Doppler shift according to (7), folded by the experimental set-up response function and presented in the same figure by the lines. All the cross sections and angles are expressed in the reaction center of mass. The fact that a part of the anisotropy should have its origin in the fragment γ-ray emission was taken into account in the theoretical spectra (lines in Fig. 5) by introducing in the code CASCADE the angular distribution of the fragment dipole γ-rays with respect to the rotational axis. To this aim, the angle dependent strength function of the dipole components is deduced from the (9) and (14):

$$f_i(\theta, E_\gamma) = f_i(E_\gamma)[1 + Q_2 a_2 P_2(\cos\theta)] \qquad (15)$$

with a coefficient a_2 for stretched and unstretched dipole transitions equal to that expected in the high spin limit, valid in the case of deep inelastic heavy-ion collisions. Q_2 is an attenuation factor for the finite γ -ray counter assumed here to have axial symmetry [57]. For the present geometry Q_2 is found to be 0.94. Moreover, fluctuations of the nuclear orientation relative to the rotation axis are neglected.

In these calculations only the fragmentation $^{75}As + ^{31}P$ was considered since it was found to largely contribute to the γ-ray spectrum. The projectile-like fragment, ^{31}P, was assumed to be spherical since its equilibrium deformation is expected to be small ($\beta_{eq} \sim 0.07$) and furthermore the $T_<$ dipole component centroid energy is expected to be high enough ($E_< = 19$ MeV) not to influence the results. The target-like fragment ^{75}As at $J \sim 26\hbar$ is expected to have an oblate non collective shape with an equilibrium deformation $\beta_{eq} \sim 0.16$. The resonance parameters corresponding to the above deformations are : $E_< = 19$ MeV, $\Gamma = 11.3$ MeV, $S_{GDR} = 1$ for the ^{31}P and $E_1 = 15.8$ MeV, $\Gamma_1 = 10$ MeV, $E_2 = 19$ MeV, $\Gamma_2 = 10$ MeV, $S_{1GDR}/S_{2GDR} = 2$ for the ^{75}As. The sum of the above lorentzian curves used for the ^{75}As can be simulated by a single lorentzian function with a centroid energy of 16.83 MeV and a width of 11 MeV. This latter allowed us to obtain a good fit of the angle integrated experimental γ-ray spectrum in the

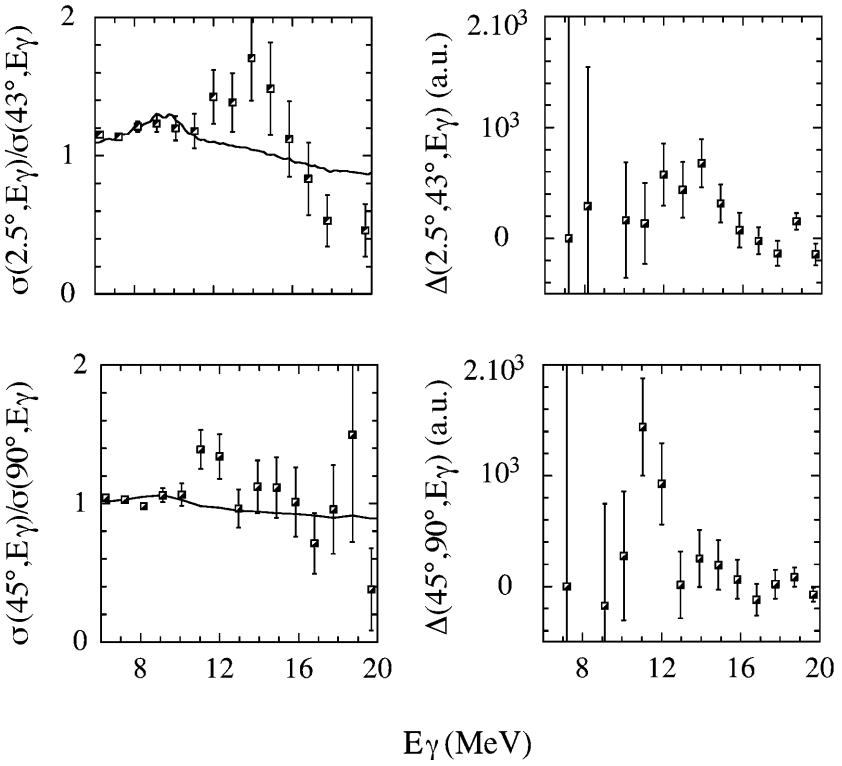

Fig. 5. Left-hand side column: the experimental γ-ray anisotropy (points) and the theoretical one calculated for the equilibrium deformation of the primary complex fragments (solid lines) and corrected for the Doppler shift. The data collected at angles θ and (180°-θ) were added and presented as $\sigma(\theta,\ E_\gamma)$ (cf. text). Right-hand side column: Difference between the same γ-ray yields as in the left-hand side column corrected for the post-fragmentation contribution from the primary fragments (cf. text). All quantities are in the reaction center of mass

analysis performed within the statistical model framework (cf. Sect. 4).

From Fig. 5, one can see that the anisotropy observed at E_γ = 10 - 15 MeV cannot be explained by the anisotropic γ-ray emission calculated for the equilibrium deformation of the primary complex fragments. In the approximation that it is exclusively due to the target-like fragment anisotropic γ-ray emission one can calculate the deformation needed to reproduce the data.

By using the same ingredients as previously, it was shown that both the γ-ray yields at 45° and 90° and the anisotropy are reasonably reproduced by using for the ^{75}As a collective prolate deformation $\beta = 0.47$ or an oblate non collective one of $\beta = 0.5$. In Fig. 6 the data obtained at 45° and 90° (two upper panels) and their ratio (lower panel) are reported with the points. The solid lines correspond to the statistical calculations made by assuming an anisotropic γ-ray emission from the ^{75}As, considered to have a prolate deformation $\beta = 0.47$ and to rotate collectively, the dashed lines correspond to an oblate non collective shape with $\beta = 0.5$ and the dotted lines to the equilibrium deformation. The resonance parameters used for obtaining the solid line are : E_1 = 13 MeV, Γ_1 = 6 MeV, E_2 = 19 MeV, Γ_2 = 10 MeV, $S_{2GDR}/S_{1GDR} = 2$ and for the dashed line : E_1 = 14 MeV, Γ_1 = 6 MeV, E_2 = 22 MeV, Γ_2 = 10 MeV, $S_{1GDR}/S_{2GDR} = 2$. The ratio of the statistical γ-ray spectra calculated at 45° and 90° in the different hypotheses is shown by the lines in the lower panel of the Fig. 6.

At the considered temperature, T ∼2.5 MeV, the target-like fragment can have a large most probable deformation because of the thermal fluctuations of its nuclear surface. However, according to the fluctuation theory [52], the γ-ray angular distribution data do not evidence its most probable deformation but a deformation which is smaller and approximately equal to the deformation of the equilibrium shape. That occurs because the enhancement of the a_2 parameter due to the thermal shape fluctuations is counteracted, especially for oblate shapes, by the suppression due to orientation fluctuations, so that the observed a_2 is an indirect indication of the equilibrium shape. With the above analysis, where orientation fluctuations have not been taken into account, the deduced target-like fragment deformation, β_{eq} ∼0.5, required to reproduce the experimental anisotropy is too large compared with its expected equilibrium deformation of β_{eq} ∼0.16. An equilibrium deformation of β_{eq} ∼0.5, extracted from the γ-ray angular distribution data, results in a larger most probable nuclear deformation which is quite unexpected for the target-like fragment at the present experimental conditions. Therefore, we conclude that the observed anisotropy cannot originate exclusively in the target-like fragment anisotropic γ-ray emission.

7 Discussion II

While for the ^{75}As and fragments in this mass region it is difficult to conceive such a large equilibrium deformation, for the intermediate system this is normally expected. Then, a way to obtain a γ-ray anisotropy at E_γ ∼12 MeV is by considering also the pre-equilibrium dipole emission from the deformed intermediate system.

To this aim, the experimental γ-ray energy spectrum measured at an angle θ relative to the rotational axis can

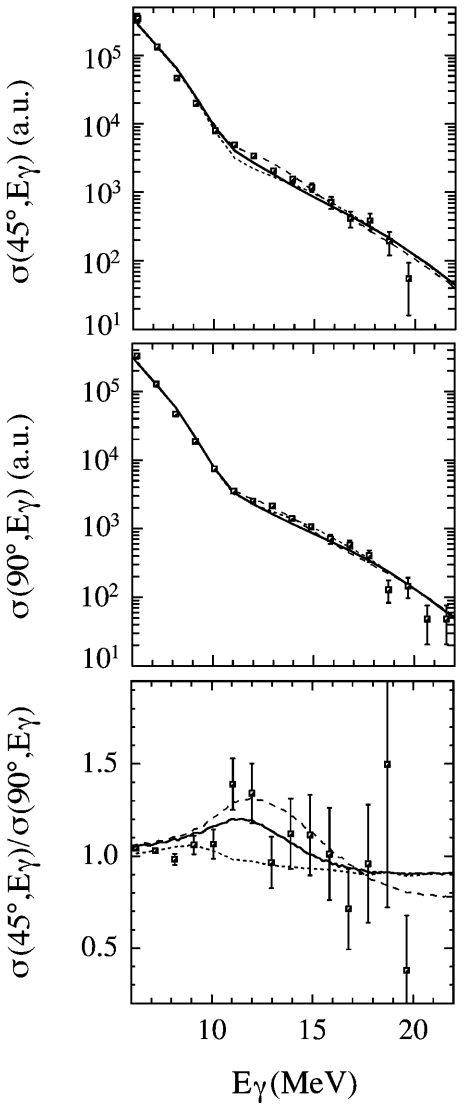

Fig. 6. Data obtained at 45° and 90° (points) in the center of mass and statistical γ-ray spectra calculated for the same geometry in the hypothesis of a prolate collective shape of the target-like fragment with $\beta = 0.47$ (solid lines), oblate non collective with $\beta = 0.5$ (dashed lines) and for the equilibrium deformation (dotted lines). Lower panel: experimental γ-ray anisotropy (points) and theoretical one calculated in the above hypotheses. The data collected at angles θ and (180°- θ) were added and presented as $\sigma(\theta, E_\gamma)$ (cf. text)

be written as the sum of two terms:

$$\sigma_{\exp}(\theta, E_\gamma) = \sigma_{pre}(\theta, E_\gamma) + \sigma_{post}(\theta, E_\gamma) \qquad (16)$$

with $\sigma_{pre}(\theta, E_\gamma)$ the contribution coming from the decay of the intermediate system dipole oscillation and $\sigma_{post}(\theta, E_\gamma)$ the post-fragmentation contribution due to the statistical γ-decay of the excited primary fragments. The latter can be evaluated for the equilibrium deformation of the fragments, introducing in the code CASCADE the angle dependent dipole component strength function given by (15) and taking into account the correction for the Doppler

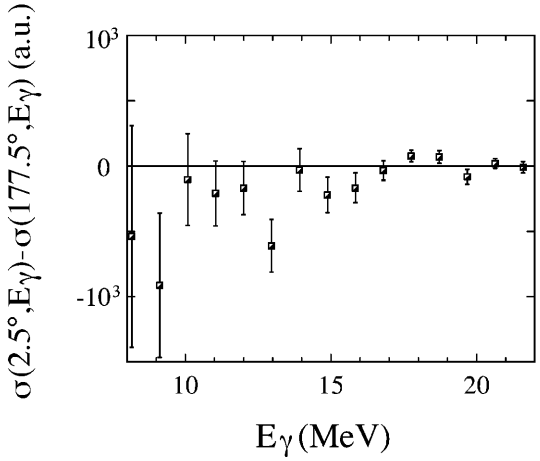

Fig. 7. Difference between the center of mass γ-ray yield collected at angles $\theta = 2.5°$ and 177.5°

shift. All quantities in (16) are in the reaction center of mass.

The center of mass energy dependent angular correlation of the dipole γ-rays emitted from the intermediate system can be written:

$$\sigma_{pre}(\theta, E_\gamma) = \sigma_{0,pre}(E_\gamma)[1 + Q_2 a_2(E_\gamma) P_2(\cos\theta)] \qquad (17)$$

The fact that (17) is used for describing the dinucleus contribution is justified from the comparison between the data collected at the same azimuthal angle and at center of mass polar angles $\theta = 2.5°$ and 177.5°. We remind that in a charge asymmetric system a part of the dipole photons should be emitted at the first moments of the dinucleus creation when the coherence of the reaction amplitudes is expected to be still strong. This assumption along with the existence of opposite parity nuclear states at the considered excitation energy imply an asymmetric center of mass γ-ray fragment angular correlation around $\theta = 90°$ which results in a difference between the γ-ray yields measured at angles θ and (180°- θ). As the difference, reported in Fig. 7, is found to be almost zero within the error bars, (17) can be applied for the γ-rays originating from the dinucleus. Actually, it is not clear whether the above result is simply due to the low statistics of the measurement or it is indeed the case. If confirmed, it could mean that most of the dipole photons are emitted at a moment when the degree of equilibrium attained from the dinucleus, though not being complete, is sufficient for the coherence between the reaction amplitudes to be lost.

Therefore, by using the (17) the difference between two experimental γ-ray spectra collected at different angles and corrected for the post fragmentation statistical contribution can be written:

$$\begin{aligned} &\sigma_{\exp}(\theta_1, E_\gamma) - \sigma_{\exp}(\theta_2, E_\gamma) \\ &-\sigma_{post}(\theta_1, E_\gamma) + \sigma_{post}(\theta_2, E_\gamma) \\ &= \Delta(\theta_1, \theta_2, E_\gamma) \end{aligned} \qquad (18)$$

$$\Delta(\theta_1, \theta_2, E_\gamma) = \sigma_{pre}(\theta_1, E_\gamma) - \sigma_{pre}(\theta_2, E_\gamma)$$

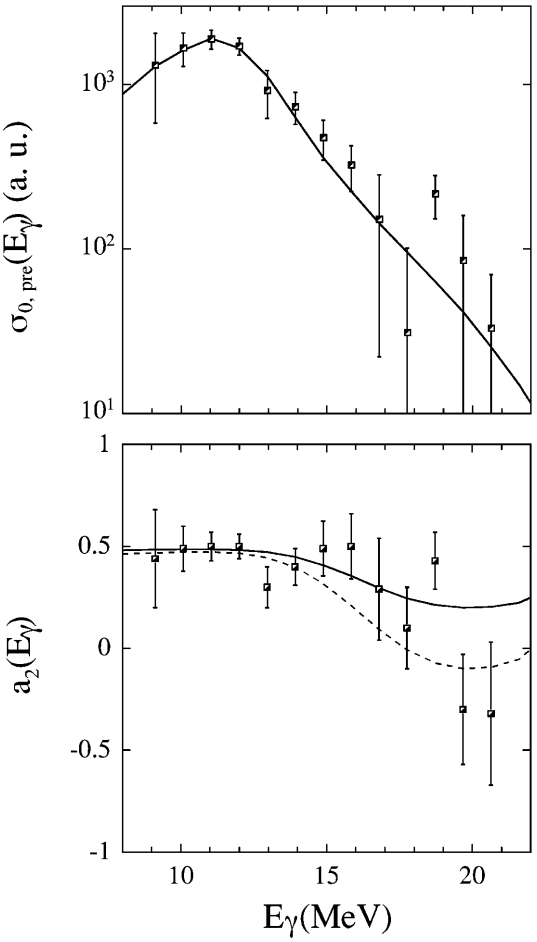

Fig. 8. $\sigma_{0,pre}(E_\gamma)$ and $a_2(E_\gamma)$ for the pre-equilibrium dipole strength (points). Upper panel: the line is a simulation of the dinucleus dipole strength by using the (20). Lower panel: the solid (dashed) line represents a calculation of the $a_2(E_\gamma)$ in the hypothesis of a prolate collective (oblate non collective) shape of the dinucleus and by using the (21) with the same parameters as for the curve of the upper panel

Two of the differences $\Delta(\theta_1,\theta_2,E_\gamma)$ are shown in the right-hand side of the Fig. 5 along with the corresponding anisotropy (left-hand side column). All the differences obtained by combining different pairs of γ-ray and fragment detectors were fitted by means of a least square procedure by using the equation:

$$\Delta(\theta_1,\theta_2,E_\gamma) = \sigma_{0,pre}(E_\gamma)[Q_2 a_2(E_\gamma)P_2(\cos\theta_1) - Q_2 a_2(E_\gamma)P_2(\cos\theta_2)] \quad (19)$$

The extracted dipole strength $\sigma_{0,pre}(E_\gamma)$ and the anisotropy $a_2(E_\gamma)$ are displayed by the points in Fig. 8.

In order to obtain informations on the pre-equilibrium dipole strength features, $\sigma_{0,pre}(E_\gamma)$ and $a_2(E_\gamma)$ were simultaneously reproduced by using the sum of three lorentzian curves multiplied by an exponential function and corrected for the experimental set up response function, as presented in Sect. 5:

$$\sigma_{0,pre}(E_\gamma) = N' \sum_i f_i(E_\gamma)\exp(-cE_\gamma) \quad (20)$$

$$a_2(E_\gamma) = \frac{0.5f_1(E_\gamma) + 0.5f_2(E_\gamma) - f_3(E_\gamma)}{\sum_i f_i(E_\gamma)} \quad (21)$$

N' is a normalization factor and $f_i(E_\gamma)$ is given by (9). In (21) orientation fluctuations of the spin axis are neglected. The parameters which best reproduce the above quantities are : $E_{GDR,low}$ = 12.5 MeV, $\Gamma_{GDR,low}$ = 4 MeV, $E_{GDR,high}$ = 19 MeV, $\Gamma_{GDR,high}$ = 8 MeV, $S_{GDR,low}/(S_{GDR,tot}) = 0.88$, $c = 1/3$ $(\mathrm{MeV})^{-1}$. The indices "low" and "high" refer to the dipole strength concentrated at the respective energies.

For reproducing $a_2(E_\gamma)$ we have two choices: a collectively rotating prolate shape (solid line of Fig. 8)

$$E_1 = 12.5\ MeV,\ \ \Gamma_1 = 4\ MeV,$$
$$E_2 = E_3 = 19\ MeV,\ \ \Gamma_2 = \Gamma_3 = 8\ MeV,$$
$$S_{1GDR}/(S_{GDR,tot}) = 0.88$$

or an oblate non collective configuration (dashed line of Fig. 8):

$$E_1 = E_2 = 12.5\ MeV,\ \ \Gamma_1 = \Gamma_2 = 4\ MeV,$$
$$E_3 = 19\ MeV,\ \ \Gamma_3 = 8\ MeV,$$
$$(S_{1GDR} + S_{2GDR})/(S_{GDR,tot}) = 0.88$$

From Fig. 8 it can be seen that $a_2(E_\gamma)$ is better reproduced in the hypothesis of a collective prolate shape. The deformation extracted from the dipole component energies is $\beta_{eq} \sim \beta = 0.5$ according to the following formula:

$$\frac{E_2}{E_1} = 0.911d + 0.089 \quad (22)$$

$$\beta = \frac{\delta}{0.95} \qquad \delta = \frac{d-1}{d^{1/3}}$$

We remind that the deduced deformation should be near to that of the equilibrium shape, therefore, the real most probable deformation of the decaying system must be larger than the obtained value. Both the deformation value and the shape of the decaying system are consistent with those expected for the dinucleus created in a deep inelastic heavy ion collision. Furthermore, the data are well reproduced with dipole component widths given by the ground state GDR data relation : $\Gamma_i = \Gamma_0 \left(\frac{E_i}{16}\right)^\delta$ with E_i the energy of the i^{th} component, $\delta \sim 1.8$ and $\Gamma_0 = 6$ MeV the width of the GDR built on the ground state of a spherical nucleus having mass $A = 106$.

The dipole strength parameters extracted from the angular correlation data analysis agree quite well with those obtained in the statistical model framework, especially when considering the total excitation energy of the primary complex fragments without any subtraction (cf. Sect. 5). Furthermore, both analyses indicate that a significant part of the total dipole strength excited in the dinucleus is concentrated at low energy.

8 Conclusions

In this work we have studied the pre-equilibrium dipole emission from the intermediate system formed in the $^{32}S + ^{74}Ge$ deep inelastic reaction. The energy spectra of the γ-rays detected in coincidence with the complex fragments were analysed in the framework of the statistical model. From this analysis it was shown that the statistical γ-ray spectra of the fragments do not fully reproduce the data since they underestimate the experimental γ-ray yield in the energy range between 10 and 15 MeV. Furthermore, in the same energy region the experimental γ-ray fragment angular correlation evidences a strong anisotropy which, according to the fluctuation theory [52], is indicative of the equilibrium deformation of the decaying nucleus. The analysis pointed out that the experimental γ-ray anisotropy is consistent with an equilibrium deformation of $\beta_{eq} \sim 0.5$ resulting in a larger most probable deformation of the nucleus. Such an exotic shape is quite unexpected for the complex fragments while it is reasonable for the intermediate system produced in a peripheral collision. Therefore, the γ-ray excess evidenced in the data with respect to the calculated statistical spectra of the fragments and the associated anisotropy were attributed to a dipole emission from the highly deformed composite system prior to fragmentation.

To further support this hypothesis, the center of mass energy dependent angular correlation for the dinucleus γ-rays was expressed as a Legendre polynomial series and the differences between the experimental γ-ray yields collected at different angles with respect to the nuclear spin direction were fitted by means of a least square method. This procedure allowed to extract the strength and the anisotropy of the dinucleus dipole emission as a function of the γ-ray energy. From their analysis a set of pre-equilibrium GDR parameters (energy, width, strength) was determined which is fully consistent with that obtained in the framework of the statistical model.

Both analyses indicate a high concentration of the dipole strength at $E_\gamma \approx 12$ MeV. Recent theoretical papers [11-15] suggest that the entrance channel charge asymmetry could determine a dipole moment which, at the very early stages of the collision, could enhance the strength of the low energy GDR component of the intermediate system. The γ-radiation emitted during these early moments comes from a pre-equilibrium stage when phase coherence between different reaction amplitudes should still be strong. In that case and if opposite parity initial nuclear states are present at the considered excitation energy, the center of mass γ-ray fragment angular correlation with respect to the nuclear spin direction should be asymmetric around $\theta = 90°$ resulting in a difference between the γ-ray yield collected at angles θ and (180°- θ). Due to the limited statistics of the single γ-ray detector cluster in the present experiment, the size of the error bars do not allow the exclusion of a symmetric angular correlation. Further investigation will be devoted to measure γ-ray angular distributions with a statistical uncertainty low enough to evidence any existing, even small, asymmetry. In this way it should be possible to understand whether and to what extent the dinucleus γ-rays originate from a rather "direct" process determined by the entrance channel charge asymmetry as suggested by the dipole strength concentration at low energy.

In the future, exotic beams could be of great interest for the study of the "direct" dipole excitation by allowing to obtain significative entrance channel charge asymmetries $\Delta(N/Z)$. In experiments where composite systems are formed with different $\Delta(N/Z)$ while keeping constant other reaction parameters, a direct comparison of the associated γ-ray spectra and angular correlations measured with high statistics should allow us to disentangle the different hypotheses.

The authors would like to thank L. Caiazzo for his assistance during the set up of the experimental apparatus.

References

1. R.G. Allas, S.S. Hanna, L. Meyer-Schutzmeister and R.E. Segel, Nucl. Phys. **58**, (1964) 122
2. K. Snover, Ann. Rev. Nucl. Part. Sci. **36**, (1986) 545
3. D.R. Chakrabarty et al., Phys. Rev. **C36**, (1987) 1886
4. A. Bracco et al., Phys. Rev. Lett. **62**, (1989) 2080 and G. Enders et al., Phys. Rev. Lett. **69**, (1992) 249
5. R. Butsch et al. Phys. Rev. **C44**, (1991) 1515 and I. Dioszegi et al. Phys. Rev. **C46**, (1992) 627
6. P. Paul and M. Thoennessen, Ann. Rev. Nucl. Part. Sci. **44**, (1994) 65
7. T.S. Tveter et al., Phys. Rev. Lett. **76**, (1996) 1035
8. T. Suomijarvi et al., Phys. Rev. **C53**, (1996) 2258
9. J.J. Gaardhoje et al., Phys. Rev. Lett. **59**, (1987) 1409
10. K. Yoshida et al., Phys. Lett. **B245**, (1990) 7 and J. Kasagi et al., Nucl. Phys **A538**, (1992) 585c
11. P.F. Bortignon, Nucl. Phys. **A583**,(1995) 101c
12. V. Baran et al., Nucl. Phys. **A600**, (1996) 111
13. D. Brink, Nucl. Phys. **A519**, (1990) 3c
14. Ph. Chomaz, M. Di Toro, A. Smerzi, Nucl. Phys. **A563**, (1993) 509
15. M. Papa et al., Eur. Phys. J. **A4**, (1999) 69
16. M. Berlanger et al., Z. Phys. **A291**, (1979) 133
17. Y. Alhassid et al., Phys. Rev. Lett. **49**, (1982) 1482
18. A. De Rosa et al., Phys. Rev. **C40**, (1989) 627
19. L. Campajola et al., Z. Phys. **A352**, (1995) 352
20. M. Sandoli et al., Z. Phys. **A357**, (1997) 67
21. A. De Rosa et al., Phys. Rev. **C44**, (1991) 747
22. L. Campajola et al., NIM **A342**, (1994) 534
23. *Treatise on Heavy-ion Science*, Vol. 2 (D.A. Bromley, Plenum Press, N.Y. 1985)
24. V.E. Viola, K. Kwiatkowski, M. Walker, Phys. Rev. **C31**, (1985) 1550
25. T.R. Davies and J.R. Nix, Phys. Rev. **C14**, (1976) 1977
26. F. Puhlhofer, Nucl. Phys. **A280**, (1977) 27 and M. N. Harakeh extended version (private communication)
27. D. Pierroutsakou et al., Nucl. Phys. **A600**, (1996) 131
28. M.N. Harakeh et al., Phys. Lett. **B176**, (1986) 297
29. S.S. Dietrich and B.L. Berman, Atomic Data and Nuclear Data Tables 38 (1988) 199
30. R.O. Akyuz and S. Fallieros, Phys. Rev. Lett. **27**, (1971) 1016

31. P. Paul, *Proceedings of the International Conference on Photonuclear Reactions and Applications*, (1973) 407
32. M. Kicinska-Habior et al., Phys. Rev. **C36**, (1987) 612
33. M. Kicinska-Habior et al., Phys. Rev. **C41**, (1990) 2075
34. S. Fallieros, B. Goulard and R. H. Venter, Phys. Lett. **19**, (1965) 398
35. S. Fallieros and B. Goulard, Nucl. Phys. **A147**, (1970) 593
36. W.E. Ormand et al., Phys. Rev. **C40**, (1989) 1510
37. A. Van der Woude, *Giant Multipole Resonances*, (1980), Nuclear Science Research Conference Series, Vol. 1, 65
38. R. Pitthan, *Nuclear Science Research Conference Series*, Vol. 1, 161
39. P. Ring and P. Schuck, *The many body problem* (Springer, Berlin) 19
40. R. Brun et al., *CERN Report No. CERN-DD/EE/84-1* (unpublished, 1986)
41. H. Nifenecker and J. A. Pinston, Annual review of nuclear and particle science **44**, (1990) 113
42. S. Cohen, F. Plasil and W.J. Swiatecki, Ann. Phys. **82**, (1974) 557 and P.F. Bortignon et al., Nucl. Phys. **A495**, (1989) 155c
43. D.R. Benton et al., Phys. Rev. **C38**, (1988) 1207
44. K. Kwiatkowski et al., Phys. Rev. **C41**, (1990) 958
45. G. Casini et al., Phys. Rev. Lett. **78**, (1997) 828
46. H. Madani et al., Phys. Rev. **C54**, (1996) 1291
47. M. Gallardo, M. Diebel, T. Dossing, R.A. Broglia, Nucl. Phys. **A443**, (1985) 415
48. D. Pierroutsakou et al., *Proc. XXXIII Int. Wint. Meet. on Nucl. Phys.* (I. Iori, Bormio 1995) 63
49. A. Bracco et al., Phys. Rev. Lett. **74**, (1995) 3748
50. S. Flibotte et al., Nucl. Phys. **A531**, (1991) 205
51. B.K. Agrawal, A. Ansari, P. Ring, Nucl. Phys. **A615**, (1997) 183
52. Y. Alhassid and B. Bush, Phys. Rev. Lett. **65**, (1990) 2527 and J.H. Gundlach et al., Phys. Rev. Lett. **65**, (1990) 2523
53. E. Ramakrishnan et al., Phys. Rev. Lett. **76**, (1996) 2025 and Nucl. Phys. A599 (1996) 49c
54. V. M. Strutinsky, Phys. Lett. **B47**, (1973) 484
55. A.Y. Abul-Magd and M. H. Simbel, Phys. Lett. **B83**, (1979) 27
56. G.R. Satchler, *Direct Nuclear Reactions*(Oxford University Press)
57. M.E. Rose, Phys. Rev. **91**, (1953) 610